Pretargeting and Bioorthogonal Click Chemistry-Mediated Endogenous Stem Cell Homing for Heart Repair

Zhenhua Li,[1,2] Deliang Shen,[3] Shiqi Hu,[1,2] Teng Su,[1,2] Ke Huang, [1,2] Feiran Liu,[1,2] Lei Hou,[,4,5] Ke Cheng*[,1,2]*

[1]Department of Molecular Biomedical Sciences and Comparative Medicine Institute, North Carolina State University, Raleigh, North Carolina 27607, USA

[2]Joint Department of Biomedical Engineering, University of North Carolina at Chapel Hill, Chapel Hill, North Carolina 27599 and North Carolina State University, Raleigh, North Carolina 27695, United States

[3]Department of Cardiology, The First Affiliated Hospital of Zhengzhou University, Zhengzhou, Henan 450052, China

[4]Department of Cardiology, Tongren Hospital, Shanghai Jiaotong University School of Medicine, Shanghai 200336, China

[5]Department of Cardiology, Shanghai Institute of Cardiovascular Diseases, Zhongshan Hospital, Fudan University, Shanghai 200433, China

Email: ke_cheng@ncsu.edu or houlei@fudan.edu.cn

Mouse Model of Myocardial Infarction (MI)

All animal work was compliant with the Institutional Animal Care and Use Committee (IACUC) of the University of North Carolina at Chapel Hill and North Carolina State University. MI models were constructed according to the procedures detailed in our previous work.[1-4] Briefly, female C57BL/6 mice (8–10 weeks old, Charles River Laboratories) were anesthetized by inhalation of 3% isoflurane in 100% oxygen, at a flow rate of 2 L·min^{-1}. Under sterile conditions, the heart was exposed by a left thoracotomy. Ischemia was created by permanent ligation of the left anterior descending coronary artery. About 30 min later, animals were given G-CSF for two days (once per day) and randomized into four treatment groups: 1) PBS; 2) DBCO-PEG-IgG; 3) G-CSF only; 4) DBCO-PEG-CD41. After a 48-hr pre-targeting interval, bioorthogonal Az-PEG-CD34 was i.v. administered. A cohort of animals was sacrificed 4 weeks after injection for heart histology.

48 hr later, Cy5-Az was utilized to detect the biodistribution of DBCO-PEG-CD41 using an IVIS imaging system after another 24 hr. Cy5-Az and PBS alone were administrated as controls. The hearts were cryo-sectioned at a thickness of 10 μm from the apex to the ligation level, with 100 μm intervals between each section. The DBCO groups in the heart were detected using FAM-Az. In addition, cell retention was determined using Az-PEG-CD34 pre-treated EPCs and DiR labeled EPCs.

Cardiac Function Assessment

The transthoracic echocardiography procedure was performed by a cardiologist who was blinded for animal group allocation, using a Philips CX30 ultrasound system, coupled with an L15 high-frequency probe. All animals inhaled 1.5% isofluorane-oxygen anesthesia mixture in supine position at the 4-hr and 4-week time points. Hearts were imaged 2D in long-axis views at the level of the greatest left ventricular (LV) diameter. LV end-diastolic volume (LVEDV) and LV end-systolic volume (LVESV) were measured to calculate left ventricular ejection fractions (LVEFs). Ejection fraction (EF) was determined by measurements from views taken from the infarcted area. Left ventricular end-systolic dimension (LVDs), end-diastolic

dimension (LVDd) and fractional shortening (LVFS) were calculated in each echocardiogram.

Heart Morphometry

After the echocardiography study at 4 weeks, all animals were euthanized. Hearts were harvested and frozen in optimum cutting temperature (OCT) compound (Tissue-Tek). Specimens were sectioned at 10 μm thicknesses from the apex to the ligation level with 100 μm intervals between each section. Masson's trichrome staining was performed as described by the manufacturer's instructions. Images were acquired with a PathScan Enabler IV slide scanner (Advanced Imaging Concepts, Princeton, NJ). From the Masson's trichrome stained images, viable myocardium was measured in each section with NIH ImageJ software. Three selected sections were quantified for each animal.

Immunohistochemistry

Heart cryo-sections were fixed with 4% paraformaldehyde in PBS for 30 min. They were then permeabilized and blocked with Protein Block Solution (DAKO), containing 0.1% saponin, for 1 hr at room temperature. For immunostaining, the samples were incubated overnight at 4°C with the following primary antibodies diluted in the blocking solution: rabbit anti-mouse alpha sarcomeric actin antibody (1:200, ab137346, Abcam) to identify cardiomyocytes; rat anti-mouse Ki67 antibody (1:200, 151202, Biolegend) to detect proliferating cells; sheep anti-mouse vWF antibody (1:200, ab11713, Abcam) to detect endothelial cells; rat anti-mouse CD34 antibody (1:200, MA1-22646, Thermo Fisher Scientific) to detect endothelial progenitor cells; rat anti-mouse CD8 (1:200, ab22378, Abcam) to detect T cells, and rabbit anti-mouse CD68 (1:200, ab125212, Abcam) antibodies to detect macrophages. After three 10-min washes with PBS, samples were incubated for 1.5 hr, at room temperature, with fluorescent secondary antibodies, including goat anti-rabbit IgG-Alexa Fluor 594 conjugate (1:400, ab150080, Abcam), goat anti-rat IgG-Alexa Fluor 488 conjugate (1:400, ab150157, Abcam), goat anti-rabbit IgG-Alexa Fluor 488 conjugate (1:400, ab150077, Abcam), and goat anti-rabbit IgG-Alexa Fluor 594 conjugate (1:400, ab150080, Abcam), based on the isotopes of the primary antibodies.

This was followed by a 10 min submersion in 4, 6-diamidino-2-phenylindole dihydrochloride (DAPI) stain, for nucleus visualization. Slides were mounted with ProLong Gold mounting solution (Thermo Fisher Scientific) and viewed using an Olympus epi-fluorescence microscopy system. Images were analyzed using NIH ImageJ software.

Statistical analysis

All experiments were performed independently at least three times, and the results were presented as mean ± standard deviation (SD). Comparisons between any two groups were performed using a two-tailed unpaired Student's *t*-test. Comparisons among more than two groups were performed using one-way ANOVA, followed by the post hoc Bonferroni test. Single, double, and triple asterisks represent $p < 0.05$, 0.01, and 0.005, respectively; $p < 0.05$ was considered statistically significant.

REFERENCES

1. Tang, J.; Su, T.; Huang, K.; Dinh, P.-U.; Wang, Z.; Vandergriff, A.; Hensley, M. T.; Cores, J.; Allen, T.; Li, T.; Sproul, E.; Mihalko, E.; Lobo, L. J.; Ruterbories, L.; Lynch, A.; Brown, A.; Caranasos, T. G.; Shen, D.; Stouffer, G. A.; Gu, Z.; Zhang, J.; Cheng, K., Targeted Repair of Heart Injury by Stem Cells Fused With Platelet Nanovesicles. *Nat. Biomed. Eng.* **2018,** *2*, 17−26.

2. Cheng, K.; Shen, D.; Hensley, M. T.; Middleton, R.; Sun, B.; Liu, W.; De Couto, G.; Marbán, E., Magnetic Antibody-linked Nanomatchmakers for Therapeutic Cell Targeting. *Nat. Commun.* **2014,** *5*, 4880−4888.

3. Vandergriff, A.; Huang K.; Shen D; Hu S; Hensley, M. T.; Caranasos, T. G. ; Qian, L.; Cheng, K.. Targeting Regenerative Exosomes to Myocardial Infarction Using Cardiac Homing Peptide. *Theranostics* **2018**, *8*, 1869−1878.

4. Tang, J.; Cui, X.; Caranasos, T. G.; Hensley, M. T.; Vandergriff, A. C.; Hartanto, Y.; Shen, D.; Zhang, H.; Zhang, J.; Cheng, K., Heart Repair Using Nanogel-Encapsulated Human Cardiac Stem Cells in Mice and Pigs with Myocardial Infarction. *ACS Nano* **2017,** *11*, 9738−9749.
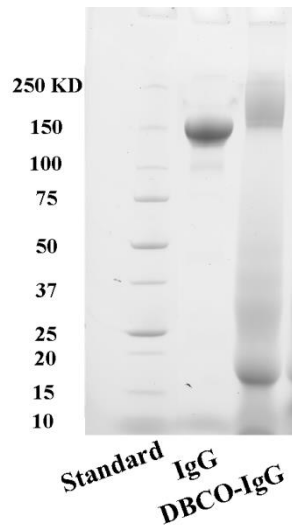
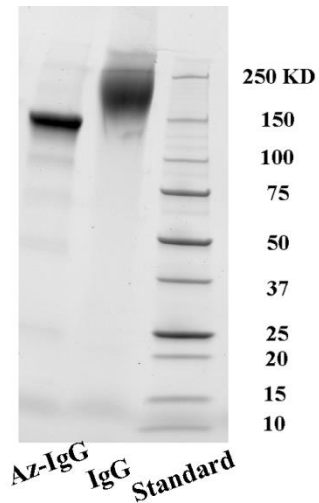**Figure S1. SDS-PAGE of IgG and DBCO-PEG-NHS-reacted IgG.**

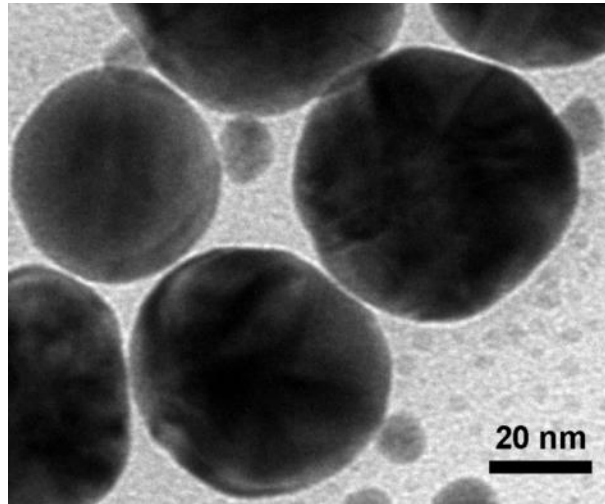**Figure S2. SDS-PAGE of IgG and Az-PEG-NHS-conjugated IgG.**

Figure S3. TEM image confirming the successful conjugation of BsAb. CD41 and CD34 antibodies derived from mice and rabbits were linked and detected by goat anti-mouse gold antibodies (40 nm) or goat anti-rabbit gold antibodies (10 nm).
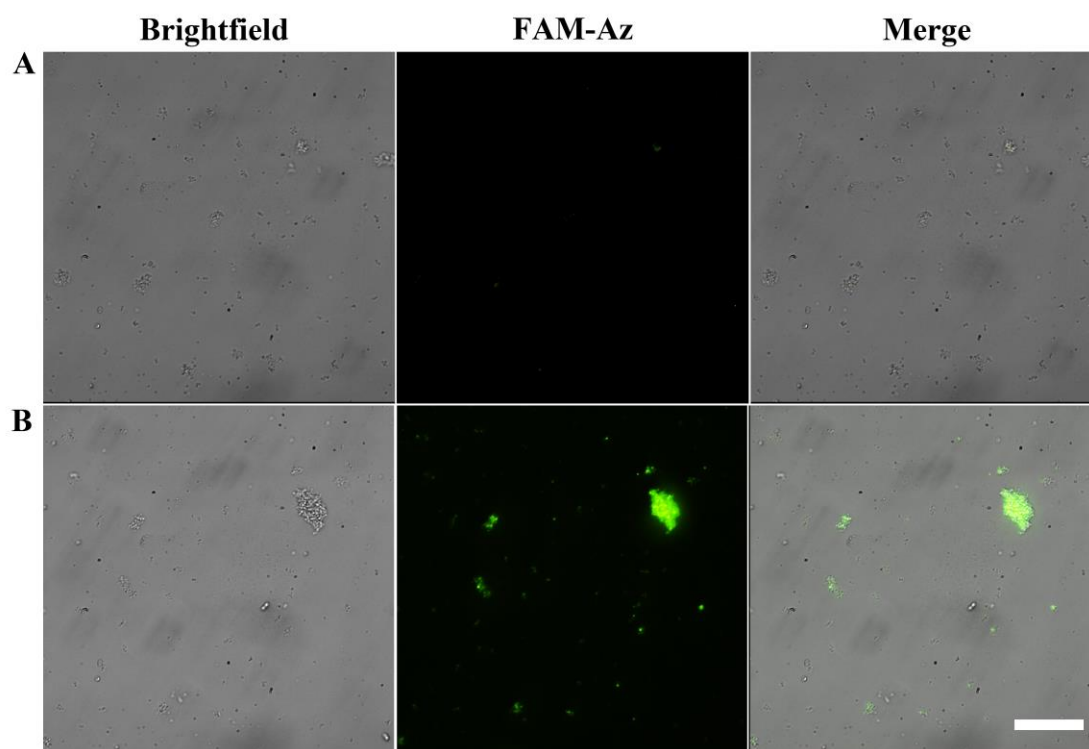
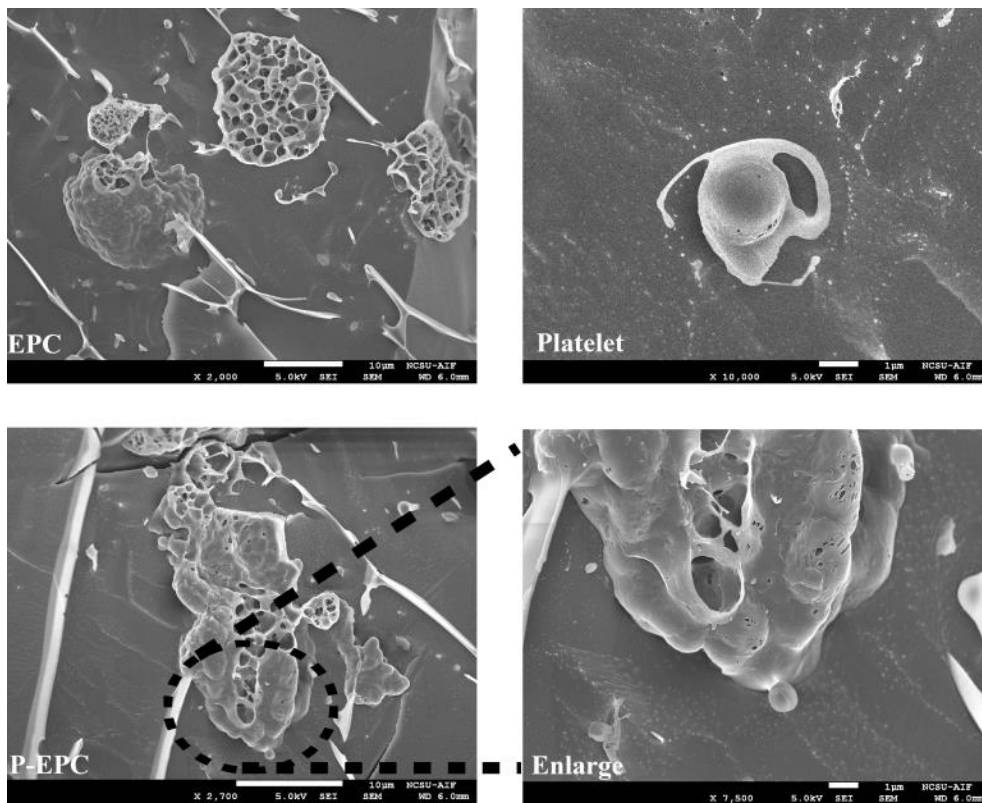**Figure S4**. **Immunofluorescent images showing DBCO-PEG-CD41-treated platelets captured by FAM-Az.** Scale bar, 10 µm.

Figure S5. SEM image showing the linking of platelets with EPCs by click reaction.
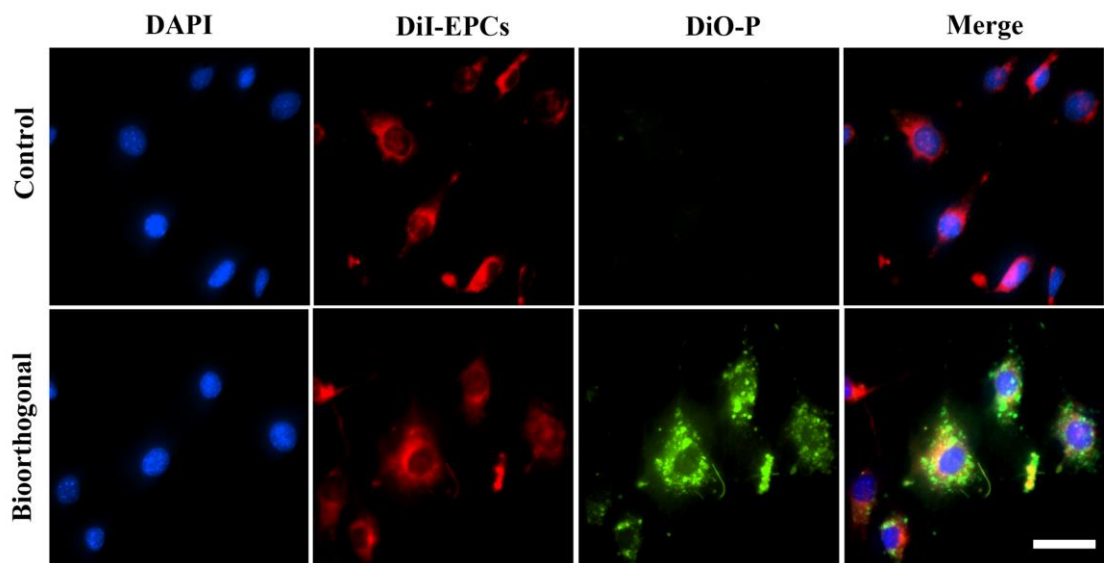
Figure S6. Confirmation of bioorthogonal conjugation of platelets with EPCs *via* DBCO-PEG-CD41 and Az-PEG-CD34. Scale bar, 10 μm.
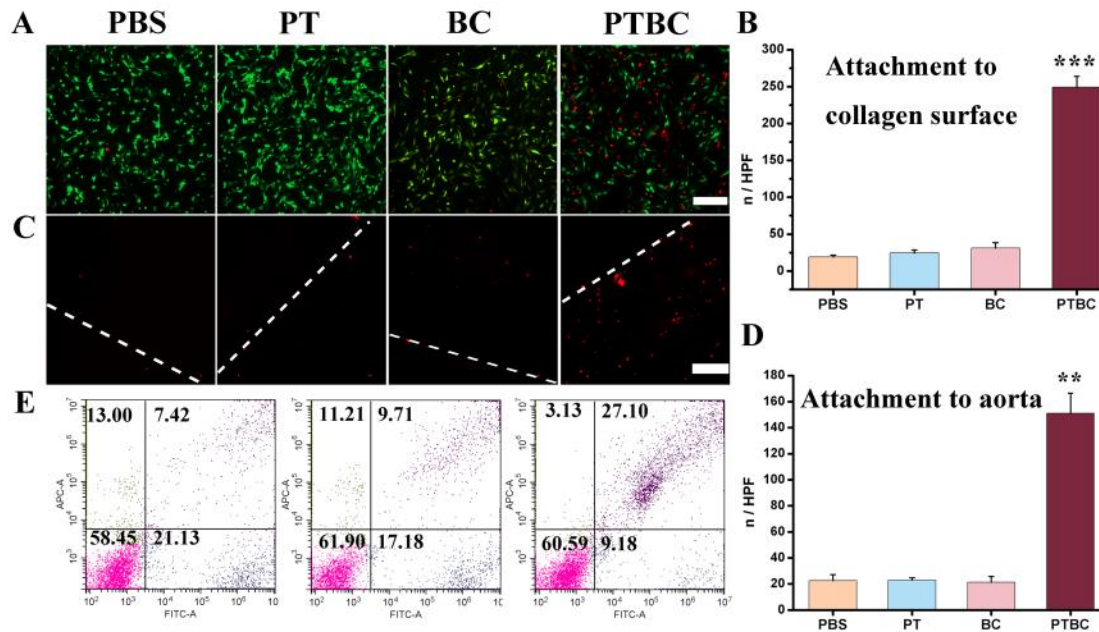
Figure S7. PTBC promotes the binding of EPCs to collagen surface and injured vasculatures. (A) Representative fluorescent images showing the binding of EPCs to collagen surfaces with HUVECs. (B) Quantitative analysis of EPC binding to collagen. (C) Representative fluorescent images showing the binding of EPCs to denuded rodent vasculatures. (D) Quantitative analysis of EPC binding to injured rodent vasculatures. (E) Flow cytometry analysis of DBCO-PEG-CD4-pretreated platelets to capture Az-PEG-CD34-pretreated EPCs in whole blood. 1×10^5 DiD-labeled Az-PEG-CD34-pretreated EPCs were mixed with whole blood and then capturing samples were added. Left to right: PBS, DiO-labeled platelets, DBCO-PEG-CD41-pretreated and DiO-labeled platelets. All data are mean ± SD. Scale bars, 100 μm. ** indicates $p < 0.01$, *** indicates $p < 0.005$.
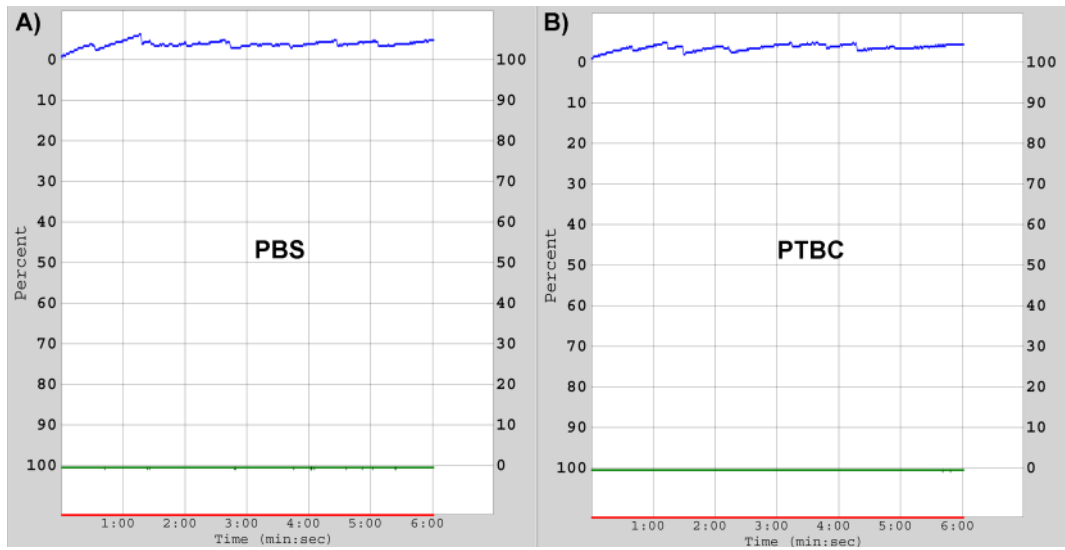
Figure S8. Aggregometry assay. (A) Whole blood was harvested and mixed with PBS. (B) Whole blood was harvested and PTBC antibodies were given.
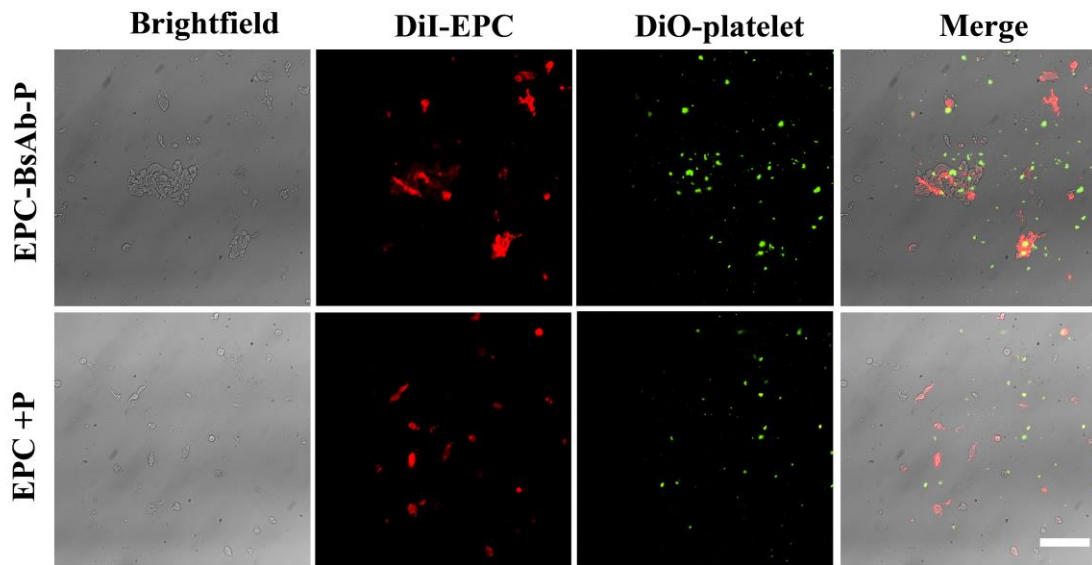

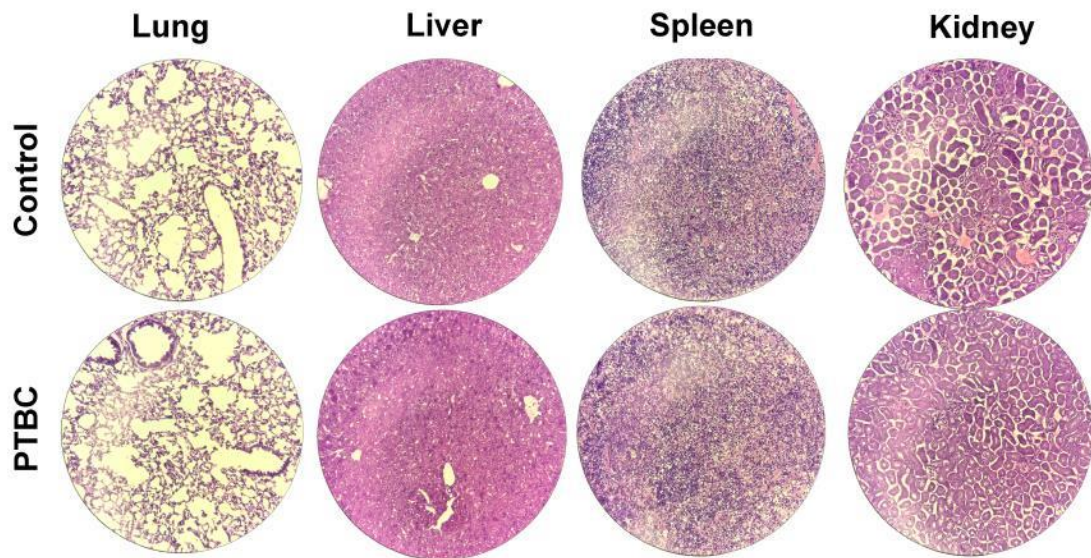**Figure S9. BsAb induces the assembly of platelets and EPCs.** Scale bar, 10 μm.

Figure S10. Toxicity of PTBC treatment. Histological assessments of major organs with H&E staining in mice 4 weeks after control or PTBC treatment. 100 x magnification.
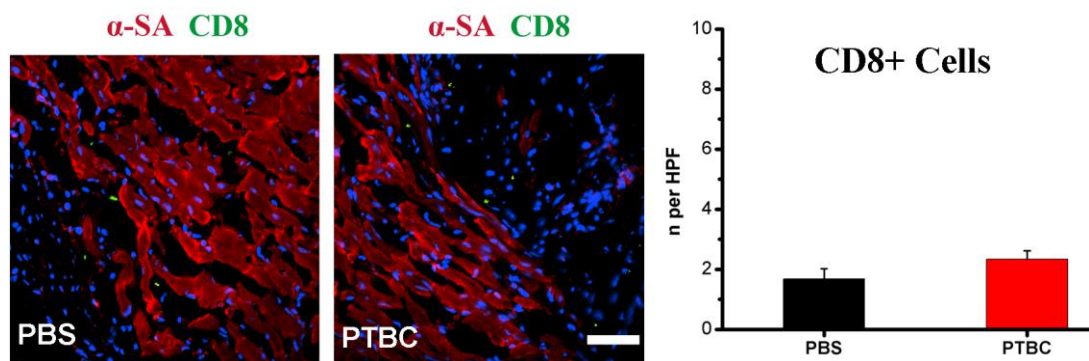

Figure S11. PTBC treatment does not cause infiltration of T cells. Microscopic images showing CD8-positive T cells in the infarct area and quantitation of cell numbers. All data are mean ± SD. Scale bar, 10 μm.
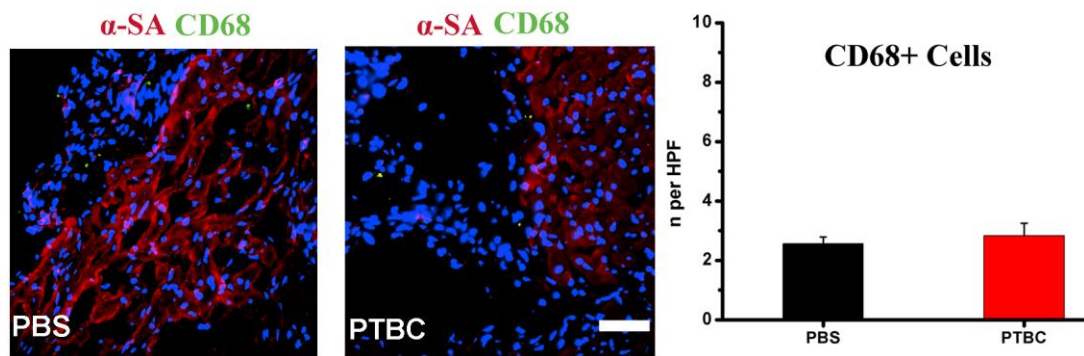
Figure S12. PTBC treatment dose not cause infiltration of macrophages. CD68-positive macrophages (magenta) in the infarct area are quantified. All data are mean ± SD. Scale bar, 10 μm.